

CAMASSA–HOLM EQUATIONS AND VORTEXONS FOR AXISYMMETRIC PIPE FLOWS

FRANCESCO FEDELE* AND DENYS DUTYKH

ABSTRACT. In this paper, we study the nonlinear dynamics of an axisymmetric disturbance to the laminar state in non-rotating Poiseuille pipe flows. In particular, we show that the associated Navier–Stokes equations can be reduced to a set of coupled Camassa–Holm type equations. These support inviscid and smooth localized travelling waves, which are numerically computed using the Petviashvili method. In physical space they correspond to localized toroidal vortices that concentrate near the pipe boundaries (wall vortexons) or wrap around the pipe axis (centre vortexons) in agreement with the analytical soliton solutions derived by Fedele (2012) for small and long-wave disturbances. Inviscid singular vortexons with discontinuous radial velocities are also numerically discovered as associated to special traveling waves with a wedge-type singularity, viz. peakons. Their existence is confirmed by an analytical solution of exponentially-shaped peakons that is obtained for the particular case of the uncoupled Camassa–Holm equations. The evolution of a perturbation is also investigated using an accurate Fourier-type spectral scheme. We observe that an initial vortical patch splits into a centre vortexon radiating vorticity in the form of wall vortexons. These can under go further splitting before viscosity dissipates them, leading to a slug of centre vortexons. The splitting process originates from a radial flux of azimuthal vorticity from the wall to the pipe axis in agreement with Eyink (2008). The inviscid and smooth vortexon is similar to the nonlinear neutral structures derived by Walton (2011) and it may be a precursor to puffs and slugs observed at transition, since most likely it is unstable to non-axisymmetric disturbances.

CONTENTS

1. Introduction	2
2. Camassa–Holm type equations for pipe flows	3
3. Is there wave dispersion in axisymmetric Navier–Stokes flows?	4
4. Long-wave limit and KdV vortexons	6
5. Regular and Singular Vortexons	7
6. Vortexon slugs	8
7. Conclusions	9
Acknowledgements	11
Appendix A. Coefficients in Camassa–Holm equations	12
Appendix B. Peakons of the dispersive CH equation	13

Key words and phrases. Navier–Stokes equations; Camassa–Holm equation; pipe flows; solitary waves; peakons.

* Corresponding author.

1. INTRODUCTION

Transition to turbulence in non-rotating pipe flows is triggered by finite-amplitude perturbations (Hof, et al. 2003), and the coherent structures observed at the transitional stage are in the form of localized patches known as puffs and slug structures (Wygnanski & Champagne 1973, Wygnanski, et al. 1975). Puffs are spots of vorticity localized near the pipe axis surrounded by laminar flow, whereas slugs expand through the entire cross-section of the pipe while developing along the streamwise direction. Recent theoretical studies related slug flows to quasi-inviscid solutions of the Navier–Stokes (NS) equations. In particular, for non-axisymmetric flows Smith & Bodonyi (1982) revealed the existence of nonlinear neutral structures localized near the pipe axis (centre modes) that are unstable equilibrium states (Walton 2005). Walton (2011) found the axisymmetric analogue of these inviscid traveling waves by studying the nonlinear stability of impulsively started pipe flows to axisymmetric perturbations. Walton’s modes are similar to the inviscid axisymmetric slug structures proposed by Smith, et al. (1990).

Recently Fedele (2012) investigated the dynamics of non-rotating axisymmetric pipe flows in terms of travelling waves of nonlinear soliton bearing equations. He showed that at high Reynolds numbers, the dynamics of small long-wave perturbations of the laminar flow obey a coupled system of nonlinear Korteweg–de Vries-type (KdV) equations. These set of equations generalize the one-component KdV model derived by Leibovich (1968) (see also Leibovich (1969), Leibovich (1984)) to study propagation of waves along the core of concentrated vortex flows (see also Benney (1966)) and vortex breakdown (Leibovich 1984). Fedele’s coupled KdV equations support inviscid soliton and periodic wave solutions in the form of toroidal vortex tubes, hereafter referred to as *vortexons*, which are similar to the inviscid nonlinear neutral centre modes found by Walton (2011). Fedele’s vortical structures eventually slowly decay due to viscous dissipation on the time scale $t \sim \mathcal{O}(\text{Re}^{6.25})$ (Fedele 2012). The vortexon, Walton’s neutral mode and the inviscid axisymmetric slug proposed by Smith et al. (1990) are similar to the slugs of vorticity that have been observed in both experiments (Wygnanski & Champagne 1973) and numerical simulations (Willis & Kerswell 2009). As discussed by Walton (2011), these inviscid structures may play a role in pipe flow transition as precursors to puffs and slugs, since most likely they are unstable to non-axisymmetric disturbances (Walton 2005).

In this paper, we extend Fedele’s analysis and show that the axisymmetric NS equations for non-rotating pipe flows can be reduced to a set of soliton bearing equations of Camassa–Holm type (Camassa & Holm 1993, Dullin, et al. 2003). These support smooth and inviscid solitary waves that are numerically computed using the Petviashvili method ((Petviashvili 1976), see also (Pelinovsky & Stepanyants 2004, Lakoba & Yang 2007, Yang 2010)) confirming the validity of the theoretical solutions derived by Fedele (2012) for long-wave disturbances. Moreover, inviscid singular solitary waves in the form of peakons are numerically discovered, and the interpretation of the associated vortical

structures are discussed. Finally, the evolution of a perturbation to the laminar state is investigated within the framework of the proposed soliton equations.

2. CAMASSA–HOLM TYPE EQUATIONS FOR PIPE FLOWS

Consider the axisymmetric flow of an incompressible fluid in a pipe of circular cross section of radius R driven by an imposed uniform pressure gradient. Define a cylindrical coordinate system (r, θ, z) with the z -axis along the streamwise direction, and (u, v, w) as the radial, azimuthal and streamwise velocity components. The time, radial and streamwise lengths as well as velocities are rescaled with T, R and U_0 respectively. Here, $T = R/U_0$ is a convective time scale and U_0 is the maximum laminar flow velocity. The Stokes streamfunction ψ of a perturbation ($u = -r^{-1}\partial_z\psi, w = r^{-1}\partial_r\psi$) to the laminar base flow $W_0(r) = 1 - r^2$ satisfies the nonlinear equation (Itoh 1977)

$$\partial_t \mathbb{L}\psi + W_0 \partial_z \mathbb{L}\psi - \frac{1}{\text{Re}} \mathbb{L}^2 \psi = \mathcal{N}(\psi), \quad (2.1)$$

where the nonlinear differential operator

$$\mathcal{N}(\psi) = -\frac{1}{r} \partial_r \psi \partial_z \mathbb{L}\psi + \frac{1}{r} \partial_z \psi \partial_r \mathbb{L}\psi - \frac{2}{r^2} \partial_z \psi \mathbb{L}\psi,$$

the linear operator

$$\mathbb{L} = \mathcal{L} + \partial_{zz}, \quad \mathcal{L} = \partial_{rr} - \frac{1}{r} \partial_r = r \partial_r \left(\frac{1}{r} \partial_r \right),$$

and Re is the Reynolds number based on U_0 and R . The boundary conditions for (2.1) reflect the boundedness of the flow at the centerline of the pipe and the no-slip condition at the wall, that is $\partial_r \psi = \partial_z \psi = 0$ at $r = 1$.

Drawing from (Fedele 2012), the solution of (2.1) can be given in terms of a complete set of orthonormal basis $\{\phi_j(r)\}$ as

$$\psi(r, z, t) = \sum_{j=1}^{\infty} \phi_j(r) B_j(z, t), \quad (2.2)$$

where B_j is the amplitude of the radial eigenfunctions ϕ_j , which satisfy the Boundary Value Problem (BVP) (Fedele, et al. 2005, Fedele 2012)

$$\mathcal{L}^2 \phi_j = -\lambda_j^2 \mathcal{L} \phi_j, \quad (2.3)$$

with $r^{-1}\phi_j$ and $r^{-1}\partial_r \phi_j$ bounded at $r = +0$, and $\phi_j = \partial_r \phi_j = 0$ at $r = 1$. Since ϕ_j satisfies the pipe flow boundary conditions *a priori*, so does ψ of (2.2). Note that the vorticity of the velocity field associated to the truncated expansion for ψ is divergence-free. The positive eigenvalues λ_j are the roots of $J_2(\lambda_j) = 0$, where $J_2(r)$ are the Bessel functions of first kind of second order (see (Abramowitz & Stegun 1972)). The corresponding eigenfunctions

$$\phi_n = \frac{\sqrt{2}}{\lambda_n} \left[r^2 - \frac{r J_1(\lambda_n r)}{J_1(\lambda_n)} \right],$$

form a complete and orthonormal set with respect to the inner product

$$\langle \varphi_1, \varphi_2 \rangle = - \int_0^1 \varphi_1 \mathcal{L}\varphi_2 r^{-1} dr = \int_0^1 \partial_r \varphi_1 \partial_r \varphi_2 r^{-1} dr.$$

A Galerkin projection of (2.1) onto the vector space \mathcal{S} spanned by the first N least stable modes $\{\phi_j\}_{j=1}^N$ yields a set of coupled Camassa–Holm (CH) type equations (Camassa & Holm 1993, Dullin et al. 2003, Dullin, et al. 2004)

$$\partial_t B_j + c_{jm} \partial_z B_m + \beta_{jm} \partial_{zzz} B_m + \alpha_{jm} \partial_{zzt} B_m + N_{jnm}(B_n, B_m) + \frac{\lambda_j^2 B_j}{\text{Re}} = 0, \quad (2.4)$$

where $j = 1, \dots, N$, the nonlinear operator

$$N_{jnm}(B_n, B_m) = F_{jnm} B_n \partial_z B_m + G_{jnm} \partial_z B_n \partial_{zz} B_m + H_{jnm} B_n \partial_{zzz} B_m, \quad (2.5)$$

the coefficients c_{jm} , β_{jm} , α_{jm} , F_{jnm} , G_{jnm} , H_{jnm} are given in A and summation over repeated indices n and m is implicitly assumed. A physical interpretation of the CH equations (2.4) is as follows: the perturbation is given by a superposition of radial structures (the eigenmodes ϕ_j) that nonlinearly interact while they are advected and dispersed by the laminar flow in the streamwise direction.

Note that CH type equations arise also as a regularized model of the 3-D NS equations (Chen, et al. 1999, Domaradzki & Holm 2001, Foias, et al. 2001, Foias, et al. 2002), the so called Navier–Stokes-alpha model.

3. IS THERE WAVE DISPERSION IN AXISYMMETRIC NAVIER–STOKES FLOWS?

The Galerkin projection described above yields the dispersive CH type equations (2.4) for the space-time evolution of the streamfunction ψ . The term $\partial_{txx}\psi$ arises also in the Benjamin–Bona–Mahony (BBM) equation (Benjamin, et al. 1972). It has the property to suppress dispersion, attenuating the dispersive effects induced by the KdV term $\partial_{xxx}\psi$. Indeed, consider the linear equation with both BBM and KdV dispersion

$$A_t - \alpha A_{xxt} + cA_x + \gamma A_{xxx} = 0.$$

The associated linear phase speed of a Fourier wave $e^{i(kx-\omega t)}$ is

$$C(k) = \frac{\omega}{k} = \frac{c - \gamma k^2}{1 + \alpha k^2},$$

and as $k \rightarrow \infty$, $C_0 \rightarrow -\gamma/\alpha$. This implies that Fourier waves with large wavenumbers tend to travel at the same speed, that is dispersion is suppressed at high k 's, if $\alpha \neq 0$. As a result, self-steepening induced by nonlinearities can become dominant and blow-up is possible in finite time, or the two contrasting effects can balance each other leading to a peakon solution (Dullin, et al. 2001, Dullin et al. 2003). The extreme case of dispersion suppression is when there is no dispersion, that is $C(k) = c$, as in the dispersionless CH equation, which also admits peakons (Camassa & Holm 1993). Clearly, if one adds a fifth-order dispersion term A_{xxxxx} , then $C(k)$ will grow as $k \rightarrow \infty$, and peakons do not exist since dispersion is too strong.

The CH/KdV dispersion is associated to a hidden ‘*elastic energy*’ that has no counterpart in axisymmetric Navier–Stokes flows, which are essentially two-dimensional (2-D) since vortex stretching is absent. To understand the physical origin of such wave dispersion, we consider the 2-D Euler equations for an inviscid fluid over the domain Ω in cartesian coordinates. The divergent-free velocity field is given by

$$\mathbf{v} = \left(-\frac{\partial \psi}{\partial y}, \frac{\partial \psi}{\partial x} \right),$$

where ψ is the streamfunction and the vorticity

$$\omega = \Delta \psi.$$

The equation of motion is

$$\frac{\partial \omega}{\partial t} = -\mathbf{v} \cdot \nabla \omega = -[\psi, \omega], \quad (3.1)$$

where the commutator

$$[f, g] = \frac{\partial f}{\partial x} \frac{\partial g}{\partial y} - \frac{\partial f}{\partial y} \frac{\partial g}{\partial x}$$

It will be useful to consider the Hamiltonian formulation of (3.1). Following Morrison (1998), this is given by

$$\frac{\partial \omega}{\partial t} = \{\omega, \mathcal{H}\}, \quad (3.2)$$

where

$$\mathcal{H} = \frac{1}{2} \int_{\Omega} |\nabla \psi|^2 \, d\Omega = -\frac{1}{2} \int_{\Omega} \omega \psi \, d\Omega.$$

is the kinetic energy of the system and the non-canonical Lie-Poisson bracket is defined as

$$\{F, G\} = \int_{\Omega} \omega \left[\frac{\delta F}{\delta \omega}, \frac{\delta G}{\delta \omega} \right] \, d\Omega,$$

where δ denotes variational derivative. Clearly, \mathcal{H} is an invariant of motion because of the anti-symmetry of the Poisson bracket, i.e. $\{F, G\} = -\{G, F\}$. The Hamiltonian structure of (3.2) yields a physical interpretation of the fluid motion in terms of a deformation of a 2-D membrane. Indeed, the Hamiltonian \mathcal{H} can be interpreted as the elastic energy of a membrane subject to tensional forces. The surface $\psi(x, y)$ represents the displacements of the deformed membrane and the vorticity ω is proportional to the mean curvature κ of ψ . This changes according to (3.2), while the elastic energy \mathcal{H} is kept invariant. As the curvature κ evolves in space and time, viz. vorticity is swept around Ω and changes in time, the surface ψ locally bends sharply if κ increases, or flattens if κ decreases. Since the velocity streamlines are the contours of ψ , this implies that the vortical flow intensifies (attenuates) in regions of high (low) curvature of ψ .

The wave dispersion associated to the ‘*elastic energy*’ \mathcal{H} can be revealed if we express (3.1) solely in terms of ψ , that is

$$\partial_t \Delta \psi = -\partial_y \psi \partial_x \Delta \psi + \partial_x \psi \partial_y \Delta \psi.$$

Here, the left-hand side yields the terms $\partial_{txx} \psi$ and $\partial_{tyy} \psi$ that are typical of the CH equation. They indicate that as the vorticity changes in time, so does the curvature κ of

the surface ψ , which elastically deforms while the ‘energy’ is conserved. If the velocity field is given by the sum of a base flow and a perturbation, then KdV type dispersive terms $\partial_{xxx}\psi$ and $\partial_{yyy}\psi$ arise from the convection of the perturbation by the mean flow.

The Navier–Stokes–alpha model can be interpreted in a similar manner (Foias et al. 2001). This is given by

$$\partial_t \mathbf{V} + \mathbf{U} \cdot \nabla \mathbf{V} + \nabla \mathbf{U}^T \cdot \mathbf{V} + \nabla p = \nu \Delta \mathbf{V}$$

$$\nabla \cdot \mathbf{U} = 0,$$

and $\mathbf{V} = (1 - \alpha^2 \Delta) \mathbf{U}$. The typical Camassa–Holm terms arise from $\partial_t \Delta \mathbf{U}$. If \mathbf{U} is the sum of a base flow and a perturbation, then KdV type dispersive terms arise as well.

4. LONG-WAVE LIMIT AND KdV VORTEXONS

As $\text{Re} \rightarrow \infty$, Fedele (2012) showed that the nonlinear dynamics of a small long-wave perturbation $b_j = \varepsilon B_j$, with $\varepsilon \sim \mathcal{O}(\text{Re}^{-2/5})$, can be reduced to that on the slow manifold of the laminar state spanned by the first few N least stable modes, and higher damped modes are neglected. This is legitimate as long as the amplitudes B_j remain small for all time and the non-resonant condition

$$\lambda_{i_1}^2 + \lambda_{i_2}^2 + \dots + \lambda_{i_k}^2 \neq \lambda_j^2 \quad (4.1)$$

is satisfied for any permutation $\{i_1, i_2, \dots, i_k\}$ of size $k \leq N$ drawn from the set $j = 1, \dots, N$ (de la Llave 1997). For the BVP of (2.3) the relation (4.1) is verified numerically to hold up to $N \cong 10^4$. For time scales much less than $t \sim \mathcal{O}(\varepsilon^{-2.5}) \cong \mathcal{O}(\text{Re}^{6.25})$, the nonlinear dynamics of (2.4) is primarily inviscid and obeys a set of coupled KdV equations (Fedele 2012)

$$\partial_\tau b_j + \tilde{\beta}_{jm} \partial_{\xi\xi\xi} b_j + \tilde{F}_{jnm} b_n \partial_\xi b_m = 0, \quad (4.2)$$

defined on the stretched reference frame

$$\xi = \varepsilon^{1/2}(z - Vt), \quad \tau = \varepsilon^{3/2}t,$$

where the tensors $\tilde{\beta}_{jm}$, \tilde{F}_{jnm} are given in Fedele (2012) and the celerity V is, with good approximation, the average of the eigenvalues of c_{jm} . The nonlinear system (4.2) support analytical travelling waves (TW), for example,

$$b_j^{(tw)}(\xi, \tau) = k^2 x_j \left[-\frac{2M^2 - 1}{3M^2} + \text{cn}(k\xi) \right], \quad (4.3)$$

where $\text{cn}(\zeta)$ is the Jacobi elliptic function with modulus $0 \leq M \leq 1$, k and M are free parameters and $\{x_j\} \in \mathbb{R}^J$ is the intersection point of J hyperconics Γ_j given by

$$-12M^2 \tilde{\beta}_{jj} x_j + \tilde{F}_{jnm} x_n x_m = 0, \quad j = 1, \dots, N.$$

For $M \rightarrow 1$, (4.3) reduces to the family of localized sech-type solitary waves

$$b_j^{(s)}(\xi, \tau) = -\frac{1}{3}k^2 x_j + k^2 x_j \text{sech}^2(k\xi). \quad (4.4)$$

In physical space, (4.3) and (4.4) represent respectively localized and periodic toroidal vortices, which travel slightly slower than the maximum laminar flow speed U_0 , *viz.* $V \approx 0.77U_0$. For $N = 2$, the vortical structures are localized near the wall (wall vortexon, x_1 and x_2 have same sign) or wrap around the pipe axis (centre vortexon, x_1 and x_2 have opposite sign). They have a non-zero streamwise mean, but they radially average to zero to conserve mass flux through the pipe. Vortexons may be related to the inviscid neutral axisymmetric slug structures discovered by Walton (2011) in unsteady pipe flows, which are similar to the centre modes proposed by Smith et al. (1990).

In the following we will compute numerically TWs of the inviscid CH-type equations (2.4) and discuss the vortical structure of the associated disturbances.

5. REGULAR AND SINGULAR VORTEXONS

Consider the inviscid three-component CH equations (2.4) with $N = 3$, and an ansatz for the wave amplitudes of the form $B_j = q + F_j(z - ct)$, where q is a free parameter and c is the velocity of the TW. The associated nonlinear steady problem for F_j (in the moving frame $z - ct$) is solved using the Petviashvili method (Petviashvili 1976), see also (Pelinovsky & Stepanyants 2004, Lakoba & Yang 2007, Yang 2010). This numerical approach has been successfully applied to derive TWs of the spatial Dysthe equation (Fedele & Dutykh 2011) and the compact Zakharov equation for water waves (Fedele & Dutykh 2012). To initialize the iterative process, the initial guess for the wave components B_j is set equal to the analytical cnoidal TW of the uncoupled KdV equations associated to (2.4), *viz.* $c_{jm} \approx c_{jj}$, $F_{jnm} \approx F_{jjj}$, and $\alpha_{jm} = G_{jnm} = H_{jnm} = 0$. Then, a converged solution is numerically continued by varying the parameters c or q . Note that the parameter that controls the strength of the nonlinearity in the truncated Camassa–Holm equations is the travelling wave amplitude.

The numerical basin of attraction of the Petviashvili scheme to localized TWs (solitons or solitary waves) is very sparse over the parameter space (c, q) . The generic topology of the flow structure associated to converged smooth TWs is the same as that of the theoretical counterpart derived by Fedele (2012): toroidal tubes of vorticity localized near the pipe boundaries (wall vortexons) or that wrap around the pipe axis (centre vortexons). In particular, wall vortexons are found in parameter window $c \sim [0.58, 0.66]$ and $q = 0$, however the Petviashvili scheme did not converge for $q > 0$. For example, for $c = 0.65$ the wave components B_j are shown in Figure 1 and the streamlines of the associated flow perturbation are reported in the top panel of Figure 2. The perturbed flow (laminar plus vortexon) is shown in the bottom panel of the same Figure. Note that wave components of higher modes have smaller amplitudes as an indication that their effects may vanish as N increases, but a more systematic numerical study of this trend is required.

Convergence to inviscid wall vortexons also occurred in the range of $c \sim [0.762, 0.79]$ and $q = 0$ (it did not converge for $q > 0$). For $c = 0.78$ the corresponding vortical structure is shown in Figure 3. Centre vortexons converged for $c \sim [0.82, 0.90]$ and $q = 0$ as depicted in Figure 4 ($c = 0.86$). In this range of values of c we note that as q increases from zero, the smooth centre vortexon bifurcates to a traveling wave with a wedge-type singularity,

viz. peakon, as shown in Figure 5 for $c = 0.90$, $q = 0.025$. In physical space the peakon corresponds to a localized vortical structure with discontinuous radial velocity u across $z - ct = 0$ (see Figure 6), but continuous streamwise velocity w since the mass flux through the pipe is conserved. As a result, a sheet of azimuthal vorticity is advected at speed c .

The Petviashvili method also converged to singular wall vortexons in the window $c \sim [0.69, 0.71]$ and only $q = 0$ as shown in Figure 7 for the case of $c = 0.70$. The existence of singular vortexons is confirmed by an analytical solution of peakons obtained for the uncoupled version of the CH equations (2.4), *viz.*

$$\partial_t B_j + c_{jj} \partial_z B_j + \beta_{jj} \partial_{zzz} B_j + \alpha_{jj} \partial_{zzt} B_j + \mathcal{N}_j(B_j) = 0, \quad (5.1)$$

where

$$\mathcal{N}_j(B_j) = F_{jjj} B_j \partial_z B_j + G_{jjj} \partial_z B_j \partial_{zz} B_j + H_{jjj} B_j \partial_{zzz} B_j,$$

and here no implicit summation over repeated indices is assumed. Note that equation (5.1) is the dispersive Camassa–Holm equation with KdV dispersion, which admits peakon solutions (Dullin et al. 2003). These are given by (see B for derivation)

$$B_j(z, t) = a_j e^{-\gamma_j |z - V_j t|}, \quad (5.2)$$

where

$$a_j = \frac{V_j \alpha_{jj} - \beta_{jj}}{H_{jjj}}, \quad V_j = \frac{c_{jj} + \beta_{jj} s_j^2}{1 + \alpha_{jj} s_j^2}, \quad \gamma_j^2 = -\frac{F_{jjj}}{G_{jjj} + H_{jjj}}.$$

Note that the peakon arises as a special balance between the linear dispersion terms $\partial_{zzz} B_j$, $\partial_{zzt} B_j$ and their nonlinear counterpart $B_j \partial_{zzz} B_j$ in (5.1). These three terms are interpreted in distributional sense because they give rise to derivatives of Dirac delta functions that must vanish by properly choosing the amplitude a_j , thus satisfying the differential equation (5.1) in the sense of distributions. The associated streamfunction $\psi_j^{(p)}$ is given by

$$\psi_j^{(p)}(r, z, t) = a_j e^{-\gamma_j |z - V_j t|} \phi_j(r).$$

For the least stable eigenmode B_1 , Figure 8 shows the remarkable agreement between the theoretical peakon (5.2) and the associated numerical solution obtained via the Petviashvili method. The associated vortical structure (streamlines) is shown in Figure 9 and it is similar to that of the numerical vortexons of Figures 6 and 7.

Finally, note that viscous dissipation precludes the existence of peakons and slowly decaying smooth vortexons appear in the CH dynamics as discussed below.

6. VORTEXON SLUGS

Hereafter, we investigate the dynamical evolution of a localized disturbance under the two-component CH dynamics with dissipation. To do so, we exploit a highly accurate Fourier-type pseudo-spectral method to solve the CH equations (2.4) as described in Fedele & Dutykh (2012)). For $\text{Re} = 8000$ Figure 10 depicts snapshots of the two-component CH solution at different times and the streamlines of the associated vortical structures are shown in Figure 11. As time evolves, the waveform of each component steepens up and then splits into solitons and radiative waves as a result of the competition between the

laminar-flow-induced wave dispersion and the nonlinear energy cascade associated to the CH nonlinearities. In physical space the initial vortical structure first compresses as a result of wave steepening and then splits into a centre vortexon and patches of vorticity in the form of wall vortexons. These may further split causing the formation of new centre and wall vortexons until viscous effects attenuate them and annihilate splitting on the time scale $t \sim \mathcal{O}(\text{Re}^{6.25})$ (Fedele 2012). The formation of a vortexon slug is clearly evident in Figure 12, in which we report the space-time plot of the difference $\beta = |B_1 - B_2|$ of the two wave components. Here, centre vortexons correspond to larger values of β (B_1 and B_2 have opposite sign), whereas smaller values of are associated to wall vortexons (B_1 and B_2 have the same sign). The centre vortexon arises due to a radial flux $F_{\theta r}^{(\omega)} \simeq u\omega_\theta$ of azimuthal vorticity ω_θ from the wall to the pipe axis. This is the mechanism of inverse cascade of cross-stream vorticity in channel flows identified by Eyink (2008). Similar dynamics is also observed for long-wave disturbances associated to the KdV equations (4.2) (Fedele & Dutykh 2013).

Note that a vortexon slug is similar to the spreading of puffs in pipe turbulence at transition (Avila, et al. 2011), but they originate from different physical mechanisms. In realistic flows, a turbulent slug arises when new puffs are produced faster than their decay in the competition between puff decay (death) and puff splitting (birth) processes. Instead, a vortexon slug arises as an inviscid competition between dispersion and nonlinear steepening of radial structures that are advected in the streamwise direction by the laminar flow.

Clearly, vortexon slugs are not the realistic slugs observed in experiments, which also have a non-axisymmetric component. However, similarly to the inviscid neutral modes found by Walton (2011), centre vortexons most likely are unstable to non-axisymmetric disturbances, and may persist viscous attenuation as precursors to puffs and slugs.

Finally, we note that observed vortex compression/splitting is also evident in the numerical simulations of the propagation of nonlinear Kelvin waves and fronts on the equatorial thermocline (Fedorov & Melville 1995, Fedorov & Melville 2000). This is expected since the geostrophic flow is two dimensional in nature and the associated dynamical equations can be reduced to KdV/CH-type models (Benney 1966).

7. CONCLUSIONS

We have shown that the axisymmetric Navier Stokes equations for non-rotating Poiseuille pipe flows can be reduced to a set of coupled Camassa–Holm type wave equations. These support inviscid and regular traveling waves that are computed numerically using the Petviashvili method. The associated flow structures are localized toroidal vortices or vortexons that travel slightly slower than the maximum laminar flow speed, in agreement with the theoretical predictions by Fedele (2012). The vortical disturbance can be localized near the wall (wall vortexon) or wrap around the pipe axis (centre vortexon). Moreover, we also discovered numerically special traveling waves with wedge-type singularities, *viz.* peakons, which bifurcate from smooth solitary waves. In physical space they correspond to localized toroidal vortical structures with discontinuous radial velocities

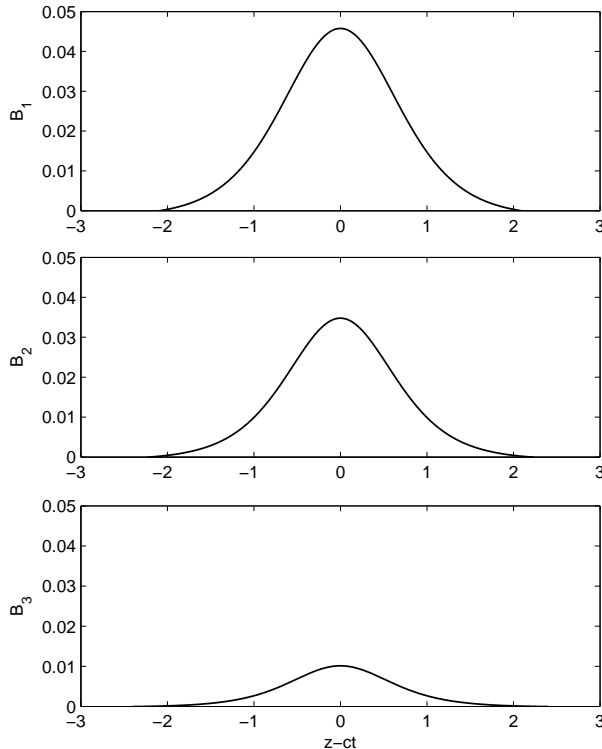


FIGURE 1. *Inviscid regular wall vortexon: wave components B_1 , B_2 and B_3 of the CH equations ($c = 0.65$, $q = 0$).*

(singular vortexon). The existence of such singular solutions is confirmed by an analytical solution of exponentially shaped peakons of the uncoupled wave equations. Clearly, the inviscid singular vortexon could be an artefact of the Galerkin truncation of the axisymmetric Euler equations that are projected onto the function space spanned by the first few Stokes eigenmodes. Viscous dissipation rules out the existence of peakons and the Camassa–Holm dynamics involves only regular vortexons. Indeed, we found numerically that an initial perturbation evolves into a vortexon slug, *viz.* a solitonic sea state of centre vortexons that split from patches of near-wall vorticity due to an inverse radial flux of azimuthal vorticity from the wall to the pipe axis in agreement with the cross-stream vorticity cascade of Eyink (2008).

Finally, we wish to emphasize the relevance of this work to the understanding of transition to turbulence. For chaotic dynamical systems the periodic orbit theory (POT) in (Cvitanović & Eckhardt 1991) and (Cvitanović 1995) interpret the turbulent motion as an effective random walk in state space where chaotic (turbulent) trajectories visit the neighborhoods of equilibria, travelling waves, or periodic orbits of the NS equations, jumping from one saddle to the other through their stable and unstable manifolds (Wedin & Kerswell 2004, Kerswell 2005, Gibson, et al. 2008). Non-rotating axisymmetric pipe flows do not exhibit chaotic behaviour (see, e.g., (Patera & Orszag 1981, Willis & Kerswell 2008)), and so the associated KdV or CH equations (even with dissipation).

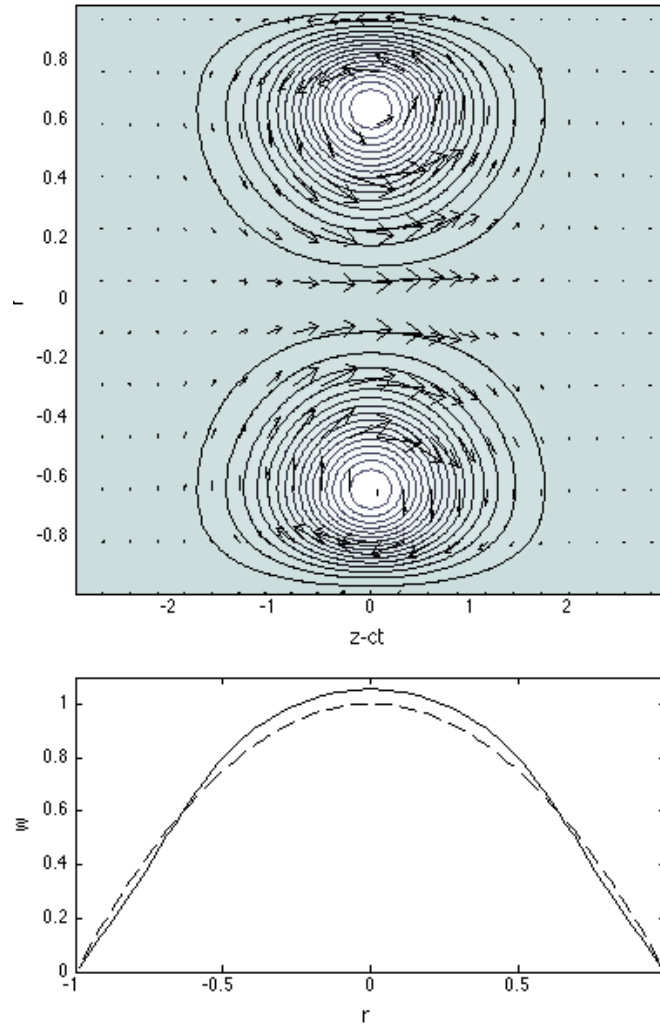


FIGURE 2. *Inviscid regular wall vortexon: (top) streamlines of the three- component CH solution of Fig. 1 and (bottom) velocity profiles of the perturbed (solid) and laminar (dash) flows ($c = 0.65$, $q = 0$).*

However, forced and damped KdV/CH equations are chaotic and the attractor is of finite dimension (see, for example, (Cox & Mortell 1986, Grimshaw & Tian 1994)). Thus, the study of the reduced KdV-CH equations associated to forced axisymmetric Navier–Stokes equations using POT may provide new insights into understanding the nature of slug flows and their formation.

ACKNOWLEDGEMENTS

F. FEDELE acknowledges the travel support received by the Geophysical Fluid Dynamics (GFD) Program to attend part of the summer school on “*Spatially Localized Structures: Theory and Applications*” at the Woods Hole Oceanographic Institution in August 2012.

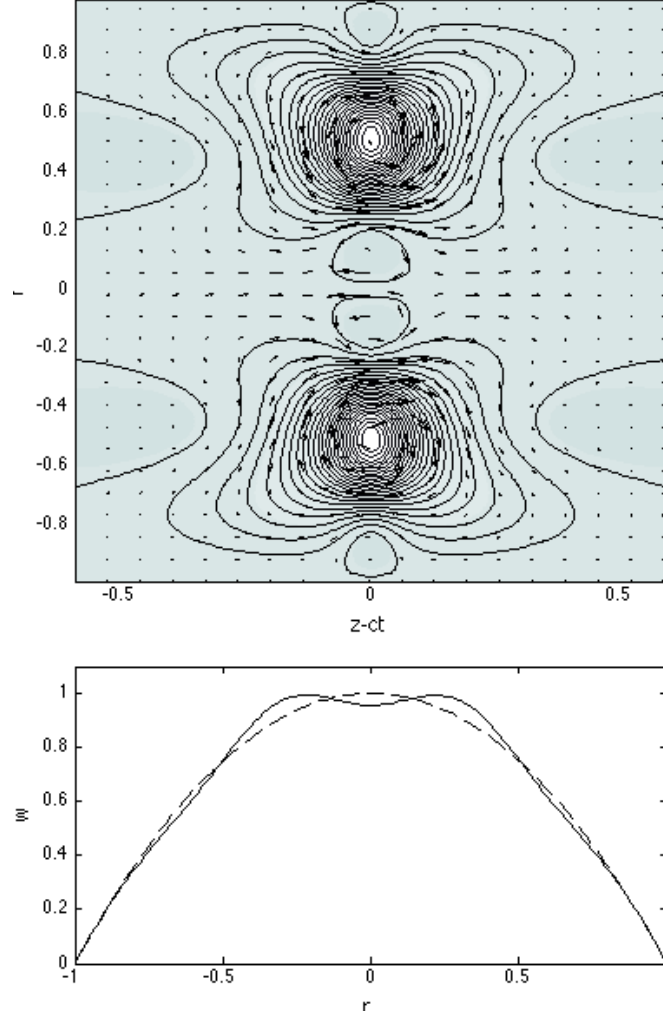


FIGURE 3. *Inviscid regular wall vortexon: (top) streamlines of the three- component CH solution for $c = 0.78$, $q = 0$, and (bottom) velocity profiles of the perturbed (solid) and laminar (dash) flows.*

D. DUTYKH acknowledges the support from ERC under the research project ERC-2011-AdG 290562-MULTIWAVE.

APPENDIX A. COEFFICIENTS IN CAMASSA–HOLM EQUATIONS

$$c_{jm} = - \int_0^1 W_0 \phi_j \mathcal{L} \phi_m r^{-1} dr, \quad \alpha_{jm} = - \int_0^1 \phi_j \phi_m r^{-1} dr, \quad \beta_{jm} = - \int_0^1 W_0 \phi_j \phi_m r^{-1} dr,$$

$$F_{jnm} = - \int_0^1 \phi_j [\partial_r \phi_n \mathcal{L} \phi_m - \partial_r (\mathcal{L} \phi_n) \phi_m + 2r^{-1} \mathcal{L} \phi_n \phi_m] r^{-2} dr,$$

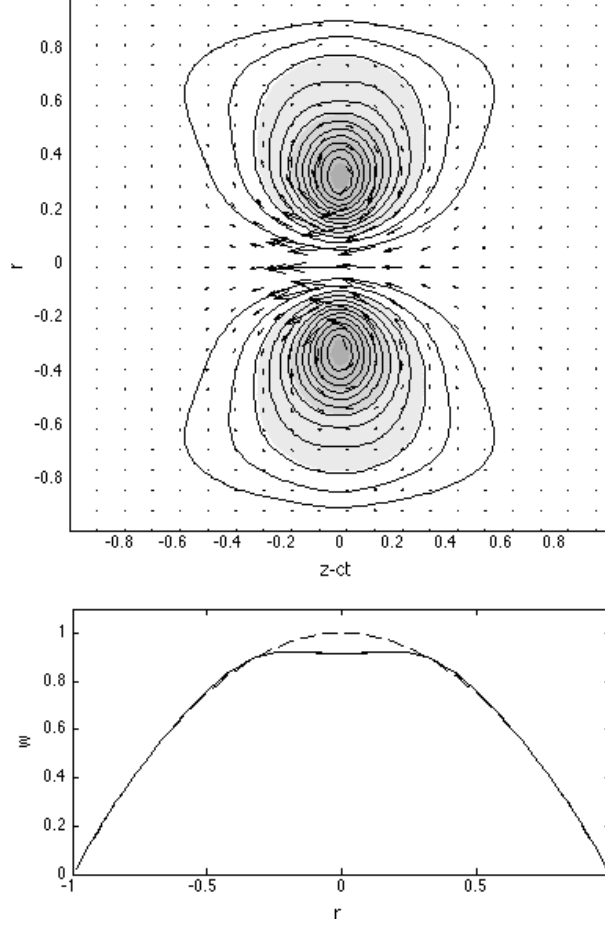


FIGURE 4. *Inviscid regular centre vortexon: (top) streamlines of the three- component CH solution for $c = 0.86$, $q = 0$, and (bottom) velocity profiles of the perturbed (solid) and laminar (dash) flows.*

$$H_{jnm} = - \int_0^1 \phi_j \phi_m \partial_r \phi_n r^{-2} dr, \quad G_{jnm} = - \int_0^1 \phi_j [-\phi_m \partial_r \phi_n + 2r^{-1} \phi_n \phi_m] r^{-2} dr.$$

APPENDIX B. PEAKONS OF THE DISPERSIVE CH EQUATION

To simplify the analysis, we drop the subscripts in (5.1) and consider

$$B_t + \alpha B_{xxt} + cB_x + \beta B_{xxx} + FBB_x + GB_x B_{xx} + HAA_{xxx} = 0. \quad (\text{B.1})$$

The ansatz for a peakon is

$$B = \begin{cases} ae^{-\gamma s(x-Vt)}, & s = 1, \quad x > Vt, \\ ae^{-\gamma s(x-Vt)}, & s = -1, \quad x < Vt, \end{cases}$$

Substituting this into (B.1) yields

$$e^{-\gamma s(x-Vt)} W_1 + e^{-2\gamma s(x-Vt)} W_2 = 0, \quad s = \pm 1,$$

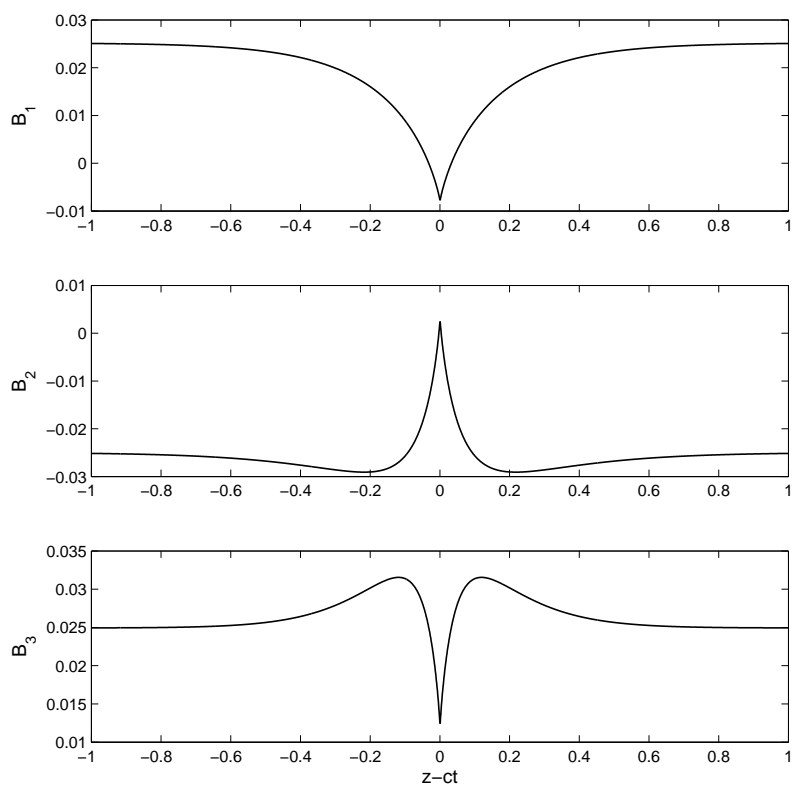


FIGURE 5. *Inviscid singular vortexon: wave components B_1 , B_2 and B_3 of the CH equations ($c = 0.90$, $q = 0.025$).*

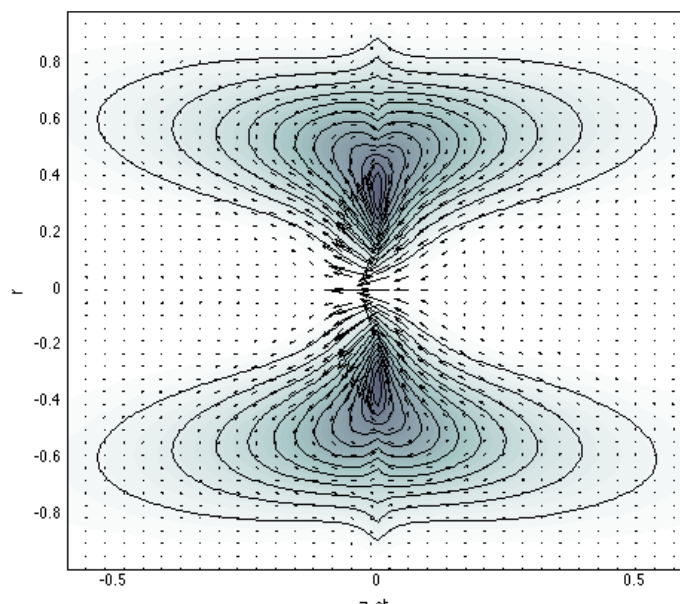


FIGURE 6. *Inviscid singular vortexon: streamlines of the three- component CH solution of Fig. 5 for $c = 0.90$, $q = 0.025$.*

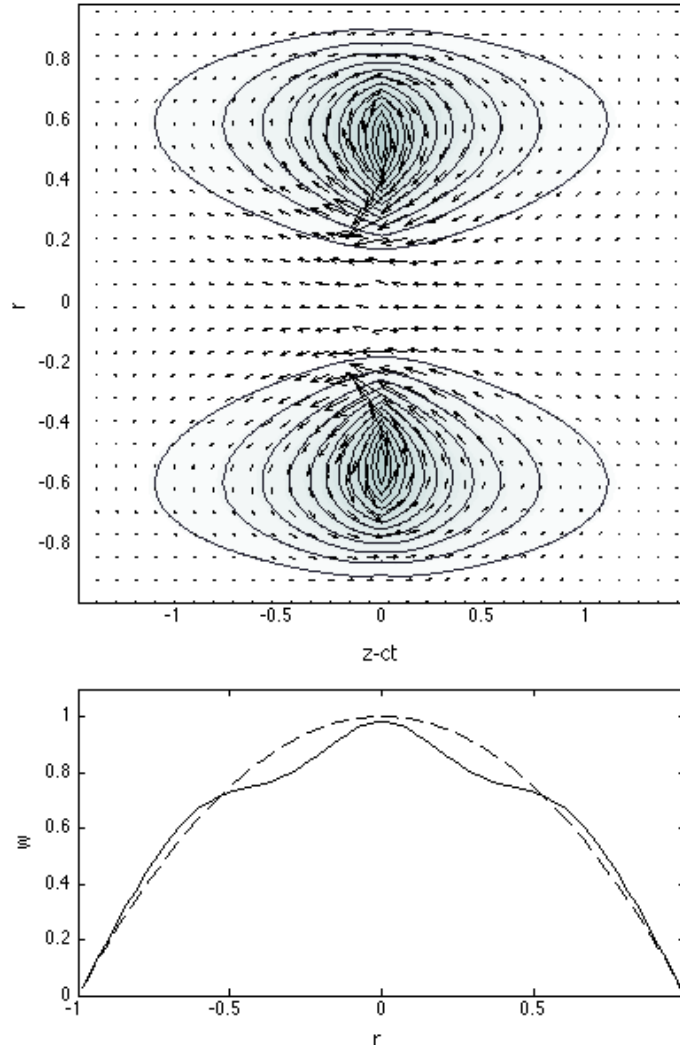


FIGURE 7. *Inviscid singular vortexon: (top) streamlines of the three- component CH solution for $c = 0.70$, $q = 0$, and (bottom) velocity profiles of the perturbed (solid) and laminar (dash) flows.*

where the coefficients W_j do not depend on s and are given by

$$W_1 = -c + V - \gamma^2(\beta - \alpha V), \quad W_2 = F + \gamma^2(G + H).$$

Imposing $W_1 = 0$ and $W_2 = 0$ yield

$$V = \frac{c + \beta\gamma^2}{1 + \alpha\gamma^2}, \quad \gamma^2 = -\frac{F}{G + H}.$$

Peakons exist if $\gamma^2 > 0$, but we still need to find their amplitude a . To do so, let us consider the general ansatz

$$B = R(\xi) = R(x - Vt),$$

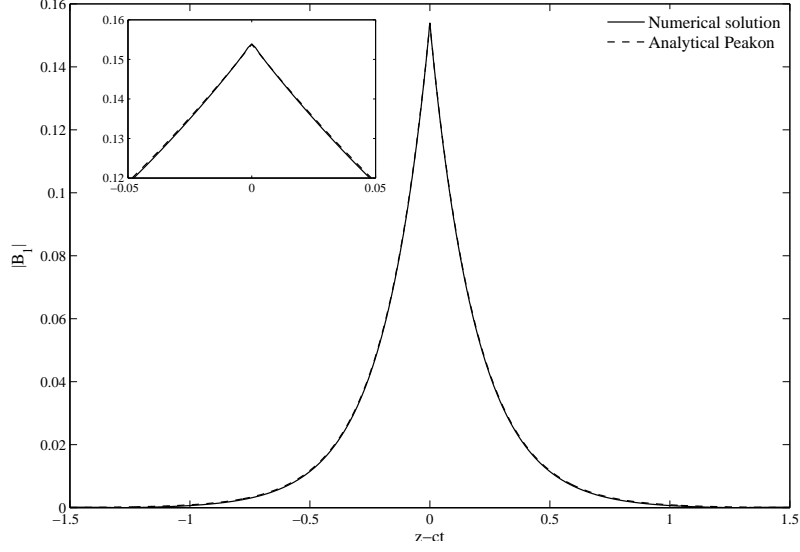


FIGURE 8. Analytical inviscid CH peakon (solid line) and numerical solution (dashed line) obtained by the Petviashvili method (dimensionless velocity $c = V_1 \approx 0.63$).

where R follows from (B.1) and it satisfies

$$-VR_\xi - \alpha VR_{\xi\xi\xi} + cR_\xi + \beta R_{\xi\xi\xi} + FRR_\xi + GR_\xi R_{\xi\xi} + HRR_{\xi\xi\xi} = 0,$$

and subscripts denote derivatives with respect to ξ . This can be written as

$$\left((c - V)R + (\beta - \alpha V + HR)R_{\xi\xi} + FR^2/2 + (G + H)R_\xi^2/2 \right)_\xi = 0. \quad (\text{B.2})$$

Clearly, if a peakon exists the term $(\beta - \alpha V + HR)R_{\xi\xi}$ must vanish at $\xi = 0$, or $x = Vt$, because it is the only distributional term in (B.2) that yields derivatives of Dirac functions. Thus, the peakon amplitude $a = R(\xi = 0) = \frac{V\alpha - \beta}{H}$.

REFERENCES

- M. Abramowitz & I. A. Stegun (1972). *Handbook of Mathematical Functions*. Dover Publications. [3](#)
- K. Avila, et al. (2011). ‘The onset of turbulence in pipe flow’. *Science* **333**(6039):192–196. [9](#)
- T. B. Benjamin, et al. (1972). ‘Model equations for long waves in nonlinear dispersive systems’. *Philos. Trans. Royal Soc. London Ser. A* **272**:47–78. [4](#)
- D. J. Benney (1966). ‘Long non-linear waves in fluid flows’. *J. Math. Phys.* **45**:52–63. [2](#), [9](#)
- R. Camassa & D. Holm (1993). ‘An integrable shallow water equation with peaked solitons’. *Phys. Rev. Lett.* **71**(11):1661–1664. [2](#), [4](#)
- S. Chen, et al. (1999). ‘The Camassa-Holm equations and turbulence in pipes and channels’. *Phys. D* **133**:49–65. [4](#)
- E. A. Cox & M. P. Mortell (1986). ‘The evolution of resonant water-wave oscillations’. *J. Fluid Mech.* **162**:99–116. [11](#)
- P. Cvitanović (1995). ‘Dynamical averaging in terms of periodic orbits’. *Phys. D* **83**(1-3):109–123. [10](#)
- P. Cvitanović & B. Eckhardt (1991). ‘Periodic orbit expansions for classical smooth flows’. *J. Phys. A: Math. Gen.* **24**(5):L237–L241. [10](#)

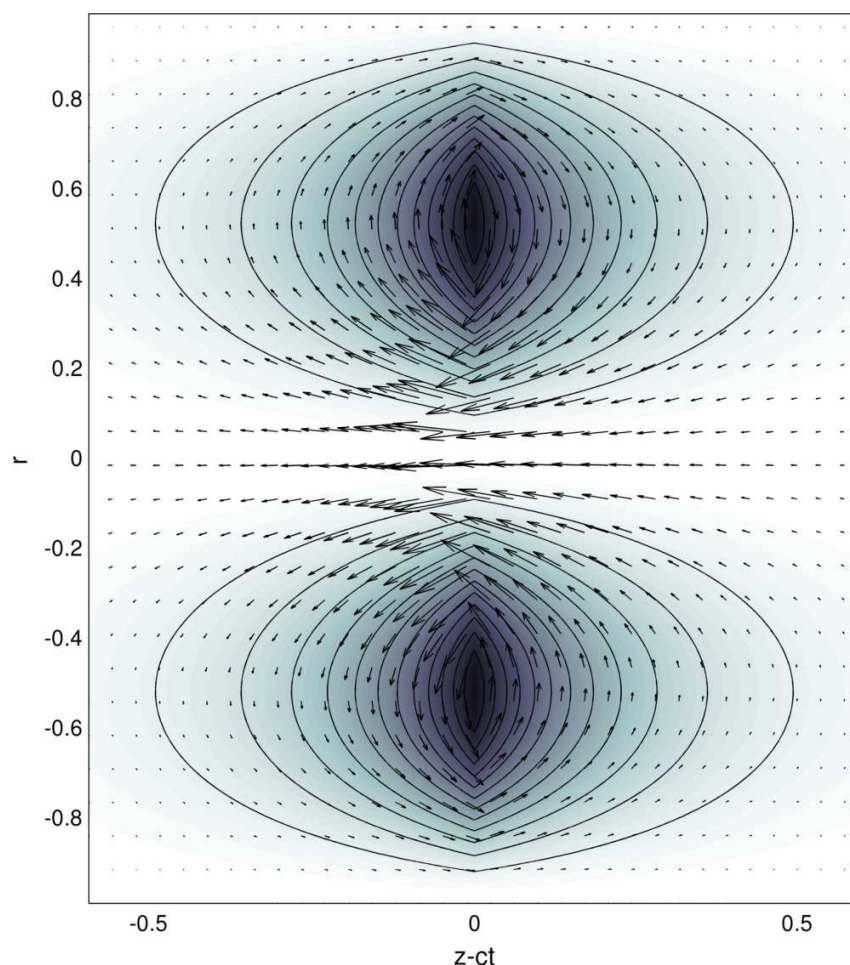


FIGURE 9. *Inviscid singular vortexon associated to the peakon of Fig. 8: streamlines of the perturbation.*

- R. de la Llave (1997). ‘Invariant manifolds associated to nonresonant spectral subspaces’. *Journal of Statistical Physics* **87**(1-2):211–249. [6](#)
- J. A. Domaradzki & D. Holm (2001). ‘Navier-Stokes-alpha model: LES equations with nonlinear dispersion’. In B. Geurts (ed.), *Modern Simulation Strategies for Turbulent Flow*, pp. 107–122. [4](#)
- H. Dullin, et al. (2001). ‘An Integrable Shallow Water Equation with Linear and Nonlinear Dispersion’. *Phys. Rev. Lett.* **87**(19):194501. [4](#)
- H. R. Dullin, et al. (2003). ‘Camassa-Holm, Korteweg-de Vries-5 and other asymptotically equivalent equations for shallow water waves’. *Fluid Dyn. Res.* **33**(1-2):73–95. [2](#), [4](#), [8](#)
- H. R. Dullin, et al. (2004). ‘On asymptotically equivalent shallow water wave equations’. *Phys. D* **190**(1-2):1–14. [4](#)
- G. L. Eyink (2008). ‘Dissipative anomalies in singular Euler flows’. *Phys. D* **237**(14-17):1956–1968. [9](#), [10](#)
- F. Fedele (2012). ‘Travelling waves in axisymmetric pipe flows’. *Fluid Dynamics Research* **44**(4):45509. [2](#), [3](#), [6](#), [7](#), [9](#)
- F. Fedele & D. Dutykh (2011). ‘Hamiltonian form and solitary waves of the spatial Dysthe equations’. *JETP Lett.* **94**(12):840–844. [7](#)
- F. Fedele & D. Dutykh (2012). ‘Special solutions to a compact equation for deep-water gravity waves’. *J. Fluid Mech* p. 15. [7](#), [8](#)

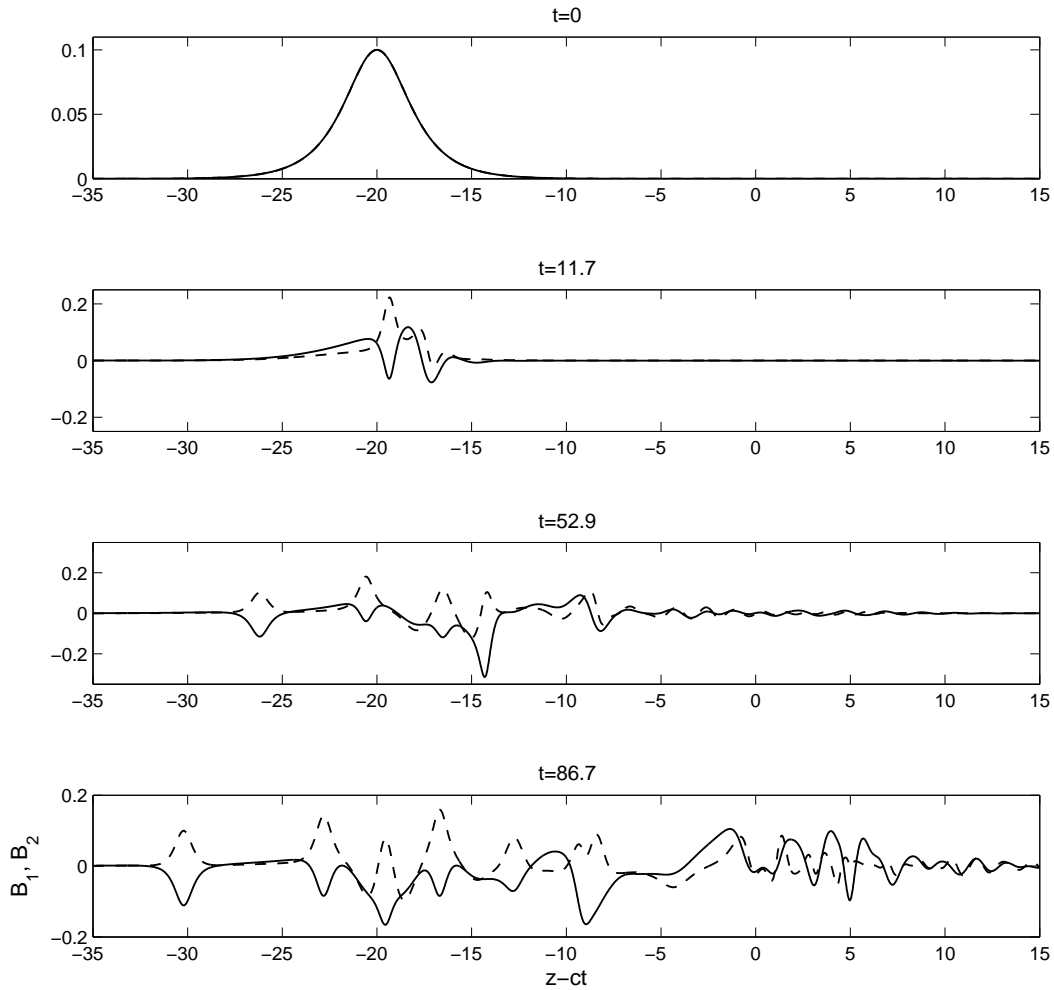


FIGURE 10. *Evolution of a perturbation under the viscous CH dynamics: wave components B_1 (solid) and B_2 (dash) at different instants of times ($\text{Re} = 8000$, speed of the reference frame $c = 0.75$).*

- F. Fedele & D. Dutykh (2013). ‘Vortexons in axisymmetric Poiseuille pipe flows’. *EPL* **101**(3):34003. [9](#)
- F. Fedele, et al. (2005). ‘Revisiting the stability of pulsatile pipe flow’. *Eur. J. Mech. B/Fluids* **24**(2):237–254. [3](#)
- A. V. Fedorov & W. K. Melville (1995). ‘Propagation and Breaking of Nonlinear Kelvin Waves’. *J. Phys. Oceanogr.* **25**(11):2518–2531. [9](#)
- A. V. Fedorov & W. K. Melville (2000). ‘Kelvin Fronts on the Equatorial Thermocline’. *J. Phys. Oceanogr.* **30**(7):1692–1705. [9](#)
- C. Foias, et al. (2001). ‘The Navier-Stokes-alpha model of fluid turbulence’. *Phys. D* **152-153**:505–519. [4, 6](#)
- C. Foias, et al. (2002). ‘The Three Dimensional Viscous Camassa-Holm Equations, and Their Relation to the Navier-Stokes Equations and Turbulence Theory’. *J. Dynam. Diff. Eqns.* **14**(1):1–35. [4](#)
- J. F. Gibson, et al. (2008). ‘Visualizing the geometry of state space in plane Couette flow’. *J. Fluid Mech.* **611**:107–130. [10](#)

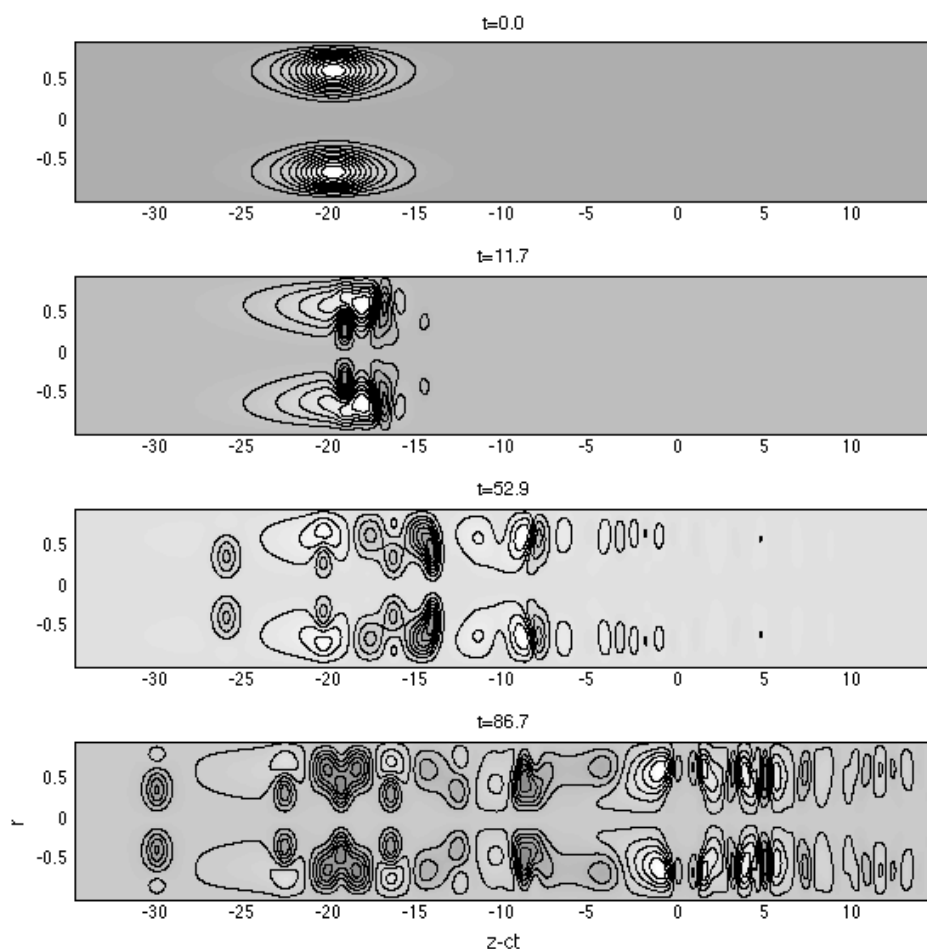


FIGURE 11. Long-time evolution of a perturbation under the viscous CH dynamics: streamlines of the vortical structures associated to the wave components of Fig. 10.

- R. Grimshaw & X. Tian (1994). ‘Periodic and Chaotic Behaviour in a Reduction of the Perturbed Korteweg-De Vries Equation’. *Proc. R. Soc. Lond. A* **445**(1923):1–21. [11](#)
- B. Hof, et al. (2003). ‘Scaling of the Turbulence Transition Threshold in a Pipe’. *Phys. Rev. Lett.* **91**(24):244502. [2](#)
- N. Itoh (1977). ‘Nonlinear stability of parallel flows with subcritical Reynolds numbers. Part 2. Stability of pipe Poiseuille flow to finite axisymmetric disturbances’. *J. Fluid Mech.* **82**(03):469–479. [3](#)
- R. R. Kerswell (2005). ‘Recent progress in understanding the transition to turbulence in a pipe’. *Nonlinearity* **18**(6):R17—R44. [10](#)
- T. I. Lakoba & J. Yang (2007). ‘A generalized Petviashvili iteration method for scalar and vector Hamiltonian equations with arbitrary form of nonlinearity’. *J. Comp. Phys.* **226**:1668–1692. [2](#), [7](#)
- S. Leibovich (1968). ‘Axially-symmetric eddies embedded in a rotational stream’. *J. Fluid Mech.* **32**(03):529–548. [2](#)
- S. Leibovich (1969). ‘Wave motion and vortex breakdown’. In *AIAA PAPER 69-645*, p. 10. [2](#)
- S. Leibovich (1984). ‘Vortex stability and breakdown - Survey and extension’. *AIAA Journal* **22**(9):1192–1206. [2](#)

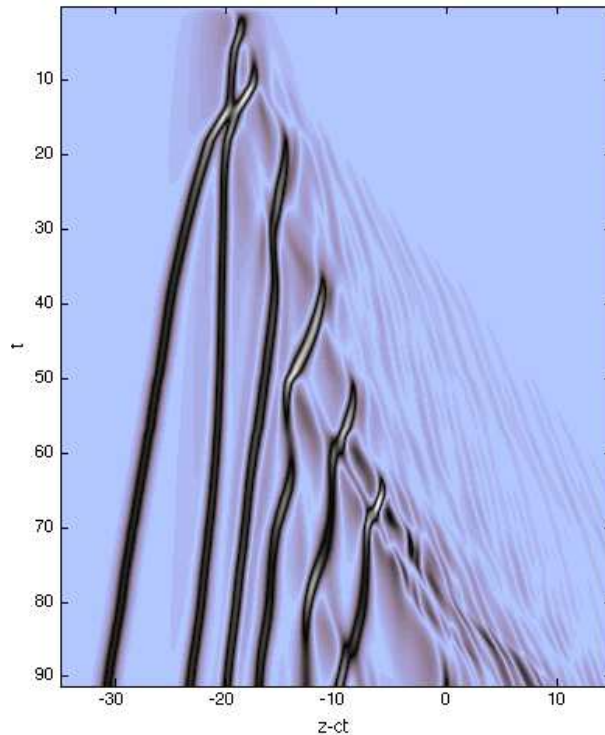


FIGURE 12. *Space-time evolution of $\beta = |B_1 - B_2|$ for $\text{Re} = 8000$, speed of the reference frame $c = 0.75$. Large values of β trace centre vortexons (B_1 and B_2 have opposite sign), whereas smaller values are associated to wall vortexons (B_1 and B_2 have same sign).*

- P. J. Morrison (1998). ‘Hamiltonian description of the ideal fluid’. *Rev. Mod. Phys.* **70**(2):467–521. [5](#)
- A. T. Patera & S. A. Orszag (1981). ‘Finite-amplitude stability of axisymmetric pipe flow’. *J. Fluid Mech.* **112**:467–474. [10](#)
- D. Pelinovsky & Y. A. Stepanyants (2004). ‘Convergence of Petviashvili’s iteration method for numerical approximation of stationary solutions of nonlinear wave equations’. *SIAM J. Num. Anal.* **42**:1110–1127. [2, 7](#)
- V. I. Petviashvili (1976). ‘Equation of an extraordinary soliton’. *Sov. J. Plasma Phys.* **2**(3):469–472. [2, 7](#)
- F. T. Smith & R. J. Bodonyi (1982). ‘Amplitude-Dependent Neutral Modes in the Hagen-Poiseuille Flow Through a Circular Pipe’. *Proc. R. Soc. Lond. A* **384**(1787):463–489. [2](#)
- F. T. Smith, et al. (1990). ‘On Displacement-Thickness, Wall-Layer and Mid-Flow Scales in Turbulent Boundary Layers, and Slugs of Vorticity in Channel and Pipe Flows’. *Proc. R. Soc. Lond. A* **428**(1875):255–281. [2, 7](#)
- A. G. Walton (2005). ‘The stability of nonlinear neutral modes in Hagen-Poiseuille flow’. *Proc. R. Soc. Lond. A* **461**(2055):813–824. [2](#)
- A. G. Walton (2011). ‘The stability of developing pipe flow at high Reynolds number and the existence of nonlinear neutral centre modes’. *J. Fluid Mech.* **684**:284–315. [2, 7, 9](#)
- H. Wedin & R. R. Kerswell (2004). ‘Exact coherent structures in pipe flow: travelling wave solutions’. *J. Fluid Mech.* **508**:333–371. [10](#)
- A. Willis & R. Kerswell (2008). ‘Coherent Structures in Localized and Global Pipe Turbulence’. *Phys. Rev. Lett.* **100**(12):124501. [10](#)

- A. P. Willis & R. R. Kerswell (2009). ‘Turbulent dynamics of pipe flow captured in a reduced model: puff relaminarization and localized ‘edge’ states’. *J. Fluid Mech.* **619**:213–233. [2](#)
- I. Wygnanski, et al. (1975). ‘On transition in a pipe. Part 2. The equilibrium puff’. *J. Fluid Mech.* **69**(02):283–304. [2](#)
- I. J. Wygnanski & F. H. Champagne (1973). ‘On transition in a pipe. Part 1. The origin of puffs and slugs and the flow in a turbulent slug’. *J. Fluid Mech.* **59**(02):281–335. [2](#)
- J. Yang (2010). *Nonlinear Waves in Integrable and Nonintegrable Systems*. Society for Industrial and Applied Mathematics. [2](#), [7](#)

SCHOOL OF CIVIL AND ENVIRONMENTAL ENGINEERING & SCHOOL OF ELECTRICAL AND COMPUTER ENGINEERING, GEORGIA INSTITUTE OF TECHNOLOGY, ATLANTA, USA

E-mail address: fedele@gatech.edu

URL: <http://savannah.gatech.edu/people/ffedele/Research/>

UNIVERSITY COLLEGE DUBLIN, SCHOOL OF MATHEMATICAL SCIENCES, BELFIELD, DUBLIN 4, IRELAND AND LAMA, UMR 5127 CNRS, UNIVERSITÉ DE SAVOIE, CAMPUS SCIENTIFIQUE, 73376 LE BOURGET-DU-LAC CEDEX, FRANCE

E-mail address: Denys.Dutykh@ucd.ie

URL: <http://www.denys-dutykh.com/>